Distinct subcellular location of the Ca^{2+}-binding protein S100A1 differentially modulates Ca^{2+}-cycling in ventricular rat cardiomyocytes

Patrick Most[1,2,*], Melanie Boerries[3,*], Carmen Eicher[2,*], Christopher Schweda[2], Mirko Völkers[2], Thilo Wedel[4], Stefan Söllner[5], Hugo A. Katus[2], Andrew Remppis[2], Ueli Aebi[3], Walter J. Koch[1] and Cora-Ann Schoenenberger[3,‡]

[1]Center for Translational Medicine, Department of Medicine, Thomas Jefferson University, Philadelphia, PA 19107, USA
[2]Department of Internal Medicine III, Division of Cardiology, University of Heidelberg, 69115 Heidelberg, Germany
[3]Maurice E. Mueller Institute, Biozentrum, University of Basel, 4056 Basel, Switzerland
[4]Institute of Anatomy and [5]Department of Plastic Surgery, University of Lübeck, 23538 Lübeck, Germany
*Authors contributed equally to this work
‡Author for correspondence (e-mail: cora-ann.schoenenberger@unibas.ch, patrick.most@jefferson.edu)

Accepted 27 October 2004
Journal of Cell Science 118, 421-431 Published by The Company of Biologists 2005
doi:10.1242/jcs.01614

Summary

Calcium is a key regulator of cardiac function and is modulated through the Ca^{2+}-sensor protein S100A1. S100 proteins are considered to exert both intracellular and extracellular functions on their target cells. Here we report the impact of an increased intracellular S100A1 protein level on Ca^{2+}-homeostasis in neonatal ventricular cardiomyocytes in vitro. Specifically, we compare the effects of exogenously added recombinant S100A1 to those resulting from the overexpression of a transduced *S100A1* gene. Extracellularly added S100A1 enhanced the Ca^{2+}-transient amplitude in neonatal ventricular cardiomyocytes (NVCMs) through a marked decrease in intracellular diastolic Ca^{2+}-concentrations ($[Ca^{2+}]_i$). The decrease in $[Ca^{2+}]_i$ was independent of sarcoplasmic reticulum Ca^{2+}-ATPase (SERCA2a) activity and was probably the result of an increased sarcolemmal Ca^{2+}-extrusion through the sodium-calcium exchanger (NCX). At the same time the Ca^{2+}-content of the sarcoplasmic reticulum (SR) decreased. These effects were dependent on the uptake of extracellularly added S100A1 protein and its subsequent routing to the endosomal compartment. Phospholipase C and protein kinase C, which are tightly associated with this subcellular compartment, were found to be activated by endocytosed S100A1.

By contrast, adenoviral-mediated intracellular S100A1 overexpression enhanced the Ca^{2+}-transient amplitude in NVCMs mainly through an increase in systolic $[Ca^{2+}]_i$. The increased Ca^{2+}-load in the SR was based on an enhanced SERCA2a activity while NCX function was unaltered. Overexpressed S100A1 colocalized with SERCA2a and other Ca^{2+}-regulatory proteins at the SR, whereas recombinant S100A1 protein that had been endocytosed did not colocalize with SR proteins. This study provides the first evidence that intracellular S100A1, depending on its subcellular location, modulates cardiac Ca^{2+}-turnover via different Ca^{2+}-regulatory proteins.

Key words: S100A1, Sodium-calcium exchanger, SERCA2a, Calcium-cycling

Introduction

S100A1 belongs to a multigenic family of small (M_r 9-13×10^3), nonubiquitous Ca^{2+}-sensing proteins of the EF-hand type. S100 proteins, which exhibit a cell- and tissue-specific expression pattern, play a major role in intracellular Ca^{2+}-homeostasis. In addition, they have been linked to the Ca^{2+}-dependent regulation of a variety of intracellular activities such as cell proliferation and differentiation or the dynamics of cytoskeletal constituents (for reviews, see Donato, 2003; Heizmann and Cox, 1998; Zimmer et al., 1995). S100A1 is the most abundant S100 protein in striated muscle and predominantly expressed in the adult heart (Haimoto and Kato, 1988; Kato and Kimura, 1985). Recent gain-of-function experiments have shown that increasing intracellular S100A1 protein levels in the adult heart and skeletal muscle resulted in enhanced Ca^{2+}-cycling and contractile function in vitro and in vivo (Most et al., 2001; Most et al., 2003b; Most et al., 2003c; Remppis et al., 2002; Remppis et al., 2004). The identification of S100A1 as a novel intracellular regulator of cardiac and skeletal muscle contractility may provide new impulses in the field of excitation-contraction coupling.

Although S100 proteins apparently lack the classic signaling sequences required for secretion, some S100 proteins seem to reach the extracellular space through secretory pathways that neither involve the common endoplasmic reticulum/Golgi nor the alternative interleukin-1 route (Rammes et al., 1997). From here, S100 proteins may exert an increasing number of downstream functions. For instance, S100B, S100A4 and S100A12 have been shown to promote differentiation of embryonic neurons (Mikkelsen et al., 2001; Novitskaya et al., 2000; Selinfreund et al., 1991). Moreover, S100B that had been secreted by astrocytes was found to be internalized by neurons,

where it influenced intracellular Ca^{2+}-levels ($[Ca^{2+}]_i$) and cellular excitability (Barger and Van Eldik, 1992; Kubista et al., 1999). Some extracellular activities of S100 proteins such as S100A12 and S100B are apparently mediated through interaction with the multiligand receptor for advanced glycation end products (RAGE) (Hofmann et al., 1999; Huttunen et al., 2000). Indeed, Roth and co-workers have shown that the S100A12/RAGE interaction plays an important role in the pathology of chronic inflammatory diseases such as bowel disease (Foell et al., 2003c), cystic fibrosis (Foell et al., 2003d), rheumatoid arthritis (Foell et al., 2003b) and vascular disorders (Foell et al., 2003a). Importantly, Donato and colleagues have shown that both RAGE-dependent and -independent extracellular effects of S100B are involved in the regulation of cell survival (Huttunen et al., 2000) and muscle development (Sorci et al., 2003; Sorci et al., 2004a; Sorci et al., 2004b). Although there is no evidence for S100A1 secretion from cardiac cells so far, a release into the extracellular space during myocardial damage has been reported (Kiewitz et al., 2000). We have recently shown that extracellularly added S100A1 is endocytosed by neonatal ventricular cardiomyocytes (NVCMs) in a RAGE-independent manner via a Ca^{2+}-dependent clathrin-mediated pathway (Most et al., 2003a). Subsequently, internalized S100A1 protected NVCMs from apoptosis via the specific activation of the extracellular signal-regulated kinase (ERK1/2) prosurvival pathway. Thus, similar to other S100 family members, S100A1 may act 'outside-in' and its extracellular presence may indicate a function as a paracrine factor in protecting the heart.

Because intracellular S100A1 plays an essential role in cardiac Ca^{2+}-handling we examined whether extracellularly added S100A1 has a similar effect on myocardial Ca^{2+}-homeostasis. The present study compares the consequences of extracellularly added S100A1 to those of virally transduced S100A1 overexpression on Ca^{2+}-cycling in NVCMs in vitro.

Materials and Methods

Reagents

Thapsigargin (T-9033), tetracaine (T-7645), monodansylcadaverine (MDC) (M-4008) and caffeine (C-0750) were purchased from Sigma. Inhibitors for protein kinase A (PKA) (myr-PKI, 476485), protein kinase C (PKC) (calphostin-c, 208725) and phospholipase C (PLC) (U-73122, 662035) were obtained from Calbiochem. NCX inhibitor myr-FRCRCF was custom-made by Eurogentec (Belgium).

Expression and purification of human recombinant S100A1 protein

Human recombinant S100A1 was produced by an isopropylthiogalactosid (IPTG)-driven expression system in *Escherichia coli* and purified as described previously (Most et al., 2003c). The coupling of S100A1 to tetramethyl-rhodamine (Rh-S100A1) was carried out by Eurogentec.

Generation of S100A1 adenovirus

The S100A1 adenovirus (AdS100A1) was generated by the use of the pAdTrack-CMV/pAdEasy-1 system as recently reported (Most et al., 2001). To facilitate identification of infected cells, AdS100A1 carried the green fluorescent protein reporter gene (GFP) in addition to the human *S100A1* cDNA (accession number X58079). Each transgene was independently expressed under the control of a cytomegalovirus promotor sequence. To rule out that the infection procedure in itself had an effect on the amount of S100A1 in the cell, NVCMs were infected with a corresponding adenovirus carrying GFP cDNA alone as a control (Adcontrol). Both replication-deficient adenoviruses were amplified in human embryonic kidney 293 cells (HEK 239), purified and enriched by cesium chloride centrifugation. Activity was tested by plaque assay.

Isolation and primary culture of neonatal rat ventricular cardiomyocytes

Ventricular cardiomyocytes from 1-2-day-old neonatal hearts (NVCMs) were prepared as published in detail elsewhere (Most et al., 2003a). NVCMs were cultured in Dulbecco's modified Eagle's medium (DMEM; Biochrom) supplemented with penicillin/streptomycin (100 units/ml), L-glutamine (2 mM), and 1% fetal calf serum (FCS Gold; PAA Laboratories GmbH; DFCS) at 37°C in a 95% air/5% CO_2 humidified atmosphere for 2-3 days. Adenoviral infection of NVCMs was carried out in serum-free HEPES-modified medium 199 (M199) with a multiplicity of infection (MOI) of 8 plaque forming units (pfu) per cell. After 4 hours incubation at 37°C in a 95% air/5% CO_2 humidified atmosphere, medium was changed to DFCS. Efficiency of adenoviral gene transfer was monitored 24 hours later by GFP fluorescence. Approximately 95% of NVCMs were infected.

Incubation of NVCMs with recombinant S100A1 (1 μM) was performed in DFCS for 24 hours and mock-treated cells served as control.

Indirect immunofluorescence

Imaging of NVCMs was carried out as described previously (Most et al., 2003a). Briefly, 3-day-old NVCMs grown on glass coverslips were treated with either Rh-S100A1 (1 μM) or S100A1 and GFP adenovirus (MOI 8 pfu/cell) as described above. After 24 hours cells were fixed, permeabilized and labeled with a polyclonal anti-S100A1 (SA 5632, Eurogentec; 1/300), a monoclonal anti-S100A1 (Sigma, 1/200), a monoclonal anti-SERCA2a (ABR) (1/500) or anti-RyR2 (ABR) (1/500) antibodies, followed by the corresponding Cy3-conjugated (Jackson ImmunoResearch Lab) (1/3000), Cy5-conjugated (Jackson ImmunoResearch Lab) (1/400) and ALEXA Fluor 488-conjugated (Alexis; 1/800) secondary antibodies. Polyclonal rabbit anti-SERCA2a antibody (1/1000) was a kind gift from F. Wuytack (Department of Molecular Cell Biology, Leuwen). Confocal images (CLSM) were obtained using a 100× oil objective on a Leica TCS SP laser scanning confocal microscope. Digitized confocal images were processed by Leica software and Adobe Photoshop.

Intracellular Ca^{2+}-calibration and Ca^{2+}-imaging in field-stimulated cardiomyocytes

Calibration and measurement of intracellular Ca^{2+}-transients in field-stimulated NVCMs using the Ca^{2+}-fluorescent dye FURA2-AM was carried out as described in detail by Most and colleagues (Most et al., 2003b). Analysis of steady state Ca^{2+}-transients at 1 Hz, 37°C and 2 mM $[Ca^{2+}]_e$ was performed with T.I.L.L. Vision software (version 4.01). Baseline data from five consecutive steady-state transients were averaged for analysis of transient amplitude (Ca^{2+} amplitude; [nM]), diastolic Ca^{2+}-levels ([nM]) and transient decay (τ; [ms]). The sarcoplasmic reticulum (SR) Ca^{2+}-load and sodium-calcium exchanger (NCX) activity were assessed by changes in the transient amplitude ([nM]) and decay (τ; [ms]), respectively, of quiescent NVCMs in modified Tyrode solution (mM: 140 NaCl, 6 KCL, 1 $MgCl_2$, 2 $CaCl_2$, 10 glucose, 5 HEPES), subjected to rapid caffeine application (10 mM) after 5 seconds rest. Exchange against sodium- and calcium-free Tyrode solution (choline chloride and EGTA replaced NaCl and $CaCl_2$, respectively) was used to block NCX

current during the decay of the caffeine-induced transient. Myr-FRCRFC (30 μM) was used to inhibit NCX current in field-stimulated NVCMs. Free intracellular Ca^{2+} concentration $[Ca^{2+}]_i$ was calculated by the equation of Grynkiewicz et al; $[Ca^{2+}]_i=K_d\times\beta\times((R-R_{min})/(R_{max}-R))$. The Ca^{2+}-transient amplitude was calculated as the difference between calibrated systolic and diastolic $[Ca^{2+}]_i$. Data sets represent analysis of 50 cells from three different preparations.

Protein expression analysis

To assess protein expression of S100A1 (Sigma) (S-2407, 1/500), sarcoplasmic reticulum Ca^{2+}-ATPase (SERCA2a; Biomol SA209, 1/5000), sodium-calcium exchanger (NCX) (ABR) (MA3-926, 1/5000) and cardiac actin (Progen Ac1-20.4.2, 1/10000), western blotting from whole-cell homogenates of NVCMs was carried out as previously described (Most et al., 2003b). Briefly, cells were washed three times with EGTA/EDTA buffer (PBS, pH 7.4, containing 2 mM EGTA/EDTA), scraped off the dish and immediately homogenized in EGTA/EDTA buffer. Homogenates were centrifuged for 10 minutes at 15,000 ***g*** and the supernatant was used for biochemical analysis. S100A1 protein was concentrated by sequential size exlusion centrifugation columns (Amicon) (Microcon YM-100 and -3).

Statistical analysis

Data are presented as mean±s.e.m. Unpaired two-tail Student's *t*-test and a two-way repeated ANOVA analysis was performed to test for differences between groups. A value of $P<0.05$ was accepted as statistically significant.

Results

Adenoviral-mediated S100A1 overexpression and endocytosis of extracellular S100A1 yield a distinct subcellular location of S100A1 in neonatal ventricular cardiomyocytes

To examine the effects of an increased S100A1 protein level on the cycling of cytosolic Ca^{2+} in neonatal rat ventricular cardiomyocytes (NVCMs), we employed two different procedures (Fig. 1): the NVCMs were either transduced by means of an adenoviral S100A1-expression construct (AdS100A1 cells, Fig. 1A) or incubated for 24 hours with DFCS containing 1 μM recombinant human S100A1 protein (Fig. 1C). As illustrated in Fig. 1, overexpressed S100A1 mainly displayed a fine granular network-like pattern. In addition, small amounts were detected in the nucleus. This pattern corresponds to the distribution of endogenous S100A1 observed in control cells (Fig. 1B). Western blotting using an antibody that reacts with both human and rat S100A1 showed that adenoviral-mediated *S100A1* gene delivery to NVCMs resulted in approximately threefold higher amounts of total S100A1 protein compared with the level of endogenous S100A1 in control cells infected with an adenoviral construct lacking the *S100A1* gene (Fig. 1A). Equivalent protein loadings were confirmed by comparable cardiac actin levels.

As an alternative approach to achieve an increase of the intracellular S100A1 level in NVCMs, we incubated cells for 24 hours in medium containing 1 μM rhodamine-coupled recombinant human S100A1 (Rh-S100A1). The CSLM image shown in Fig. 1C reveals an intracellular perinuclear accumulation of Rh-S100A1. This finding is consistent with our recently published data, which shows that following

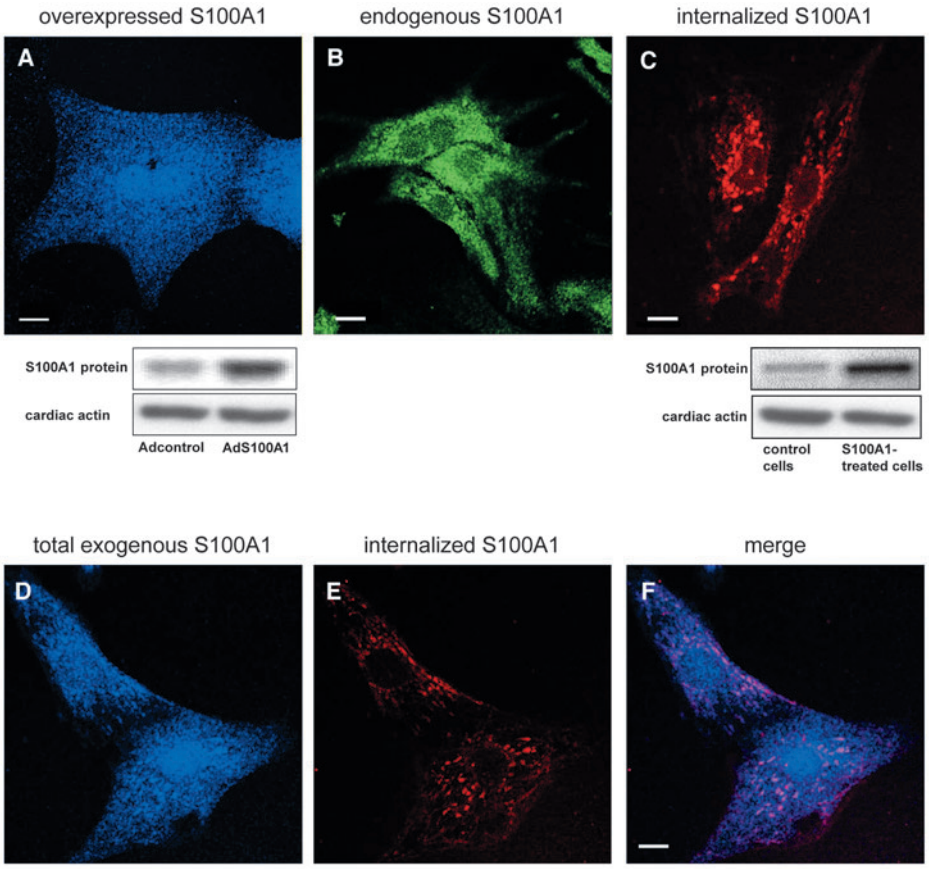

Fig. 1. Subcellular location of overexpressed, endogenous and internalized S100A1. (A) Overexpressed S100A1 (AdS100A1; blue) is detected by an antibody that specifically reacts with S100A1. Western blot analysis comparing levels of S100A1 (upper) and cardiac actin (lower) expression in homogenates of Adcontrol and AdS100A1-transduced NVCMs. (B) Immunostaining of endogenous S100A1 (green) in untreated NVCMs reveals a fine granular network-like pattern (control). (C) Vesicular accumulation of internalized Rh-S100A1 protein (red) in the perinuclear region and in the cytosol of S100A1-treated cells. Western blot analysis comparing levels of S100A1 (upper) and cardiac actin (lower) in homogenates from S100A1-treated and control NVCMs. (D-F) AdS100A1-transduced cells were incubated for 1 hour with Rh-S100A1 24 hours post infection, and then immunolabeled with an antibody that specifically reacts with human S100A1. (D) The anti-human S100A1/Cy5-anti-rabbit antibody detects internalized Rh-S100A1 as well as overexpressed S100A1 protein (total exogenous S100A1). (E) Vesicular accumulation of internalized Rh-S100A1 protein in the perinuclear region and in the cytosol. (F) Overlay of both D and F shows that internalized Rh-S100A1 (violet) exhibits a distinct distribution compared with overexpressed S100A1 (blue). Bar, 10 μm.

endocytosis via a Ca^{2+}-dependent calthrin-mediated process, the extracellularly added S100A1 is routed to the endosomal compartment (Most et al., 2003a). The uptake of S100A1 caused an almost fourfold increase of intracellular S100A1 in NVCMs compared with mock-treated control cells (Fig. 1C). To directly correlate the distribution of exogenous S100A1 resulting from the two different procedures, we incubated AdS100A1 cells for 1 hour with Rh-S100A1 protein (1 μM) 24 hours after adenoviral infection (Fig. 1D-F). As in the individually treated cells, the internalized recombinant human Rh-S100A1 (red, Fig. 1E) displayed a vesicular-like endosomal localization in AdS100A1 cells. When immunolabeled with a polyclonal antibody that specifically recognizes the hinge region of human S100A1, both S100A1 populations were recognized in the S100A1-treated AdS100A1 cells (blue, Fig. 1D). Superimposing the CSLM image of total exogenous S100A1 with the internalized Rh-S100A1 (Fig. 1F) confirmed that the localization of internalized Rh-S100A1 (violet) was clearly distinct from the fine granular network-like pattern of overexpressed human S100A1 (blue).

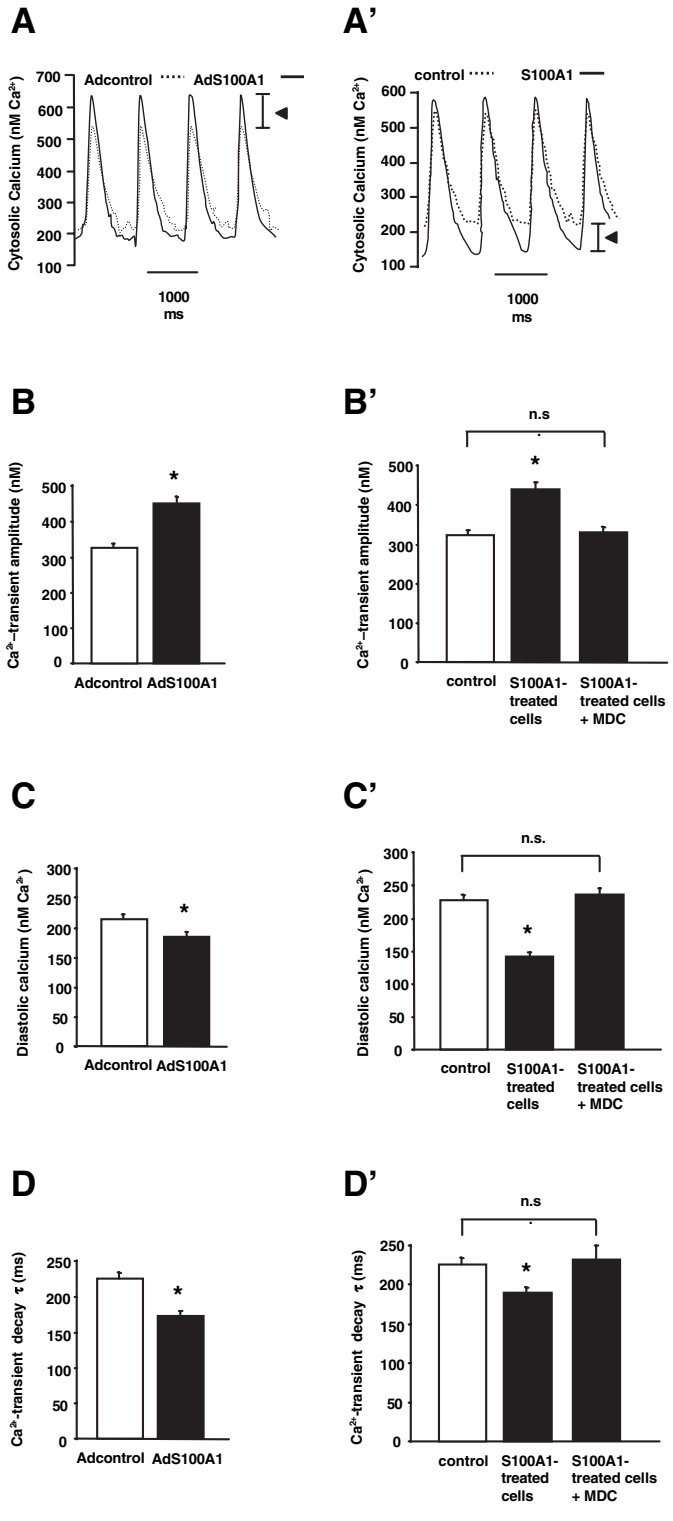

Elevated S100A1 enhances cytosolic Ca^{2+}-turnover in neonatal ventricular cardiomyocytes

As illustrated by the Ca^{2+}-transients in Fig. 2, the overexpression of S100A1 in AdS100A1-transduced NVCMs gave rise to an enhanced cytosolic Ca^{2+}-cycling compared with control cells. The overall enhanced Ca^{2+}-cycling was reflected by an increased amplitude of Ca^{2+}-transients in AdS100A1 cells (Fig. 2B). The larger amplitude was predominantly due to an S100A1-induced rise of systolic $[Ca^{2+}]_i$ as indicated by the higher peak in AdS100A1-transduced NVCMs (Fig. 2A, bar). Concomitantly, S100A1 overexpression also decreased diastolic $[Ca^{2+}]_i$ (Fig. 2C), which was associated with a reduction in the Ca^{2+}-transient decay-constant τ (Fig. 2D).

Similar to S100A1 overexpression in AdS100A1 cells, uptake of S100A1 also had an effect on the Ca^{2+}-transients recorded in S100A1-treated cells (Fig. 2A'). Accordingly, they exhibited an increased amplitude (Fig. 2B'), indicating that the rise in intracellular S100A1 caused an increased cytosolic Ca^{2+}-turnover in S100A1-treated NVCMs. However, in contrast to Ca^{2+}-transients of cells with adenoviral-mediated S100A1 overexpression, the amplitude of S100A1-treated cells was

Fig. 2. Overexpressed and internalized S100A1 enhance cytosolic Ca^{2+}-turnover in neonatal ventricular cardiomyocytes. (A-D) Adenoviral-transduced NVCMs overexpressing S100A1. (A) Superimposed tracings of calibrated Ca^{2+}-transients in S100A1-overexpressing (AdS100A1, solid line) and control (Adcontrol, dashed line) NVCMs. Note the gain in systolic $[Ca^{2+}]_i$ in S100A1-overexpressing NVCMs (bar). (B-D) Effects of increased S100A1 protein level on Ca^{2+}-transients. Compared with control cells expressing endogenous levels of S100A1, S100A1 overexpression significantly increases the Ca^{2+}-transient amplitude (AdS100A1 454±22 nM vs. Adcontrol 311±11 nM; 1B), lowers diastolic $[Ca^{2+}]_i$ (AdS100A1 181±14 nM vs. Adcontrol 219±12 nM; 1C), and accelerates the decay of the Ca^{2+}-transient (τ, AdS100A1 172±14 ms vs. Adcontrol 223±11 ms; 1D). *n*=150 cells from three different cell preparations. Data are given as mean±s.e.m. (A'-D') NVCMs treated with 1 μM human recombinant S100A1. (A') Superimposed tracings of calibrated Ca^{2+}-transients in S100A1-treated (S100A1, solid line) and mock-treated (control, dashed line) NVCMs. The decrease in diastolic $[Ca^{2+}]_i$ in S100A1-treated NVCMs is indicated by the bar. (B') S100A1-uptake increases the Ca^{2+}-transient amplitude (S100A1-treated 442±23 nM vs. control 324±15 nM). (C') The effects of an increased S100A1 level are a reduction of diastolic $[Ca^{2+}]_i$ (S100A1-treated 143±13 nM vs. control 236±14 nM) and (D') an accelerated decay of the Ca^{2+}-transient (τ, S100A1-treated 182±16 ms vs. control 232±10 ms). Pre-incubation with monodansylcadaverine (MDC, an inhibitor of clathrin-mediated endocytosis) abolished the effects of extracellularly added S100A1 on the Ca^{2+}-turnover (* $P<0.01$ vs. no inhibitor).

primarily increased by a marked reduction of diastolic $[Ca^{2+}]_i$, and to a lesser extent by elevated systolic $[Ca^{2+}]_i$ (Fig. 2A', bar and Fig. 2C'). For both, overexpression and uptake from the extracellular environment, increased S100A1 levels accelerated diastolic Ca^{2+}-elimination as indicated by a decrease in the Ca^{2+}-transient decay-constant τ (Fig. 2D and D').

To test whether binding of extracellular S100A1 to NVCMs was sufficient to induce an improved cytosolic Ca^{2+}-cycling or whether endocytosis was required, NVCMs were treated with recombinant S100A1 in the presence of monodansylcadaverine (MDC, 50 μM), which was shown to effectively prevent S100A1 uptake (Most et al., 2003a). As illustrated by the Ca^{2+}-transients, the presence of MDC precluded changes in the amplitude (Fig. 2B') and diastolic $[Ca^{2+}]_i$ (Fig. 2C') as well as in the decay of the Ca^{2+}-transient (Fig. 2D').

Together these results show that an augmented intracellular S100A1 protein level in NVCMs increases cytosolic Ca^{2+}-turnover. More specifically, we observed a differential effect of adenoviral-mediated S100A1 overexpression versus increased S100A1 following endocytosis: higher systolic Ca^{2+}-peaks were responsible for the increased amplitude of Ca^{2+}-transients in NVCMs overexpressing S100A1, whereas a marked decrease in diastolic $[Ca^{2+}]_i$ largely accounted for the increased amplitude of Ca^{2+}-transients in cells after endoyctosis of extracellular S100A1.

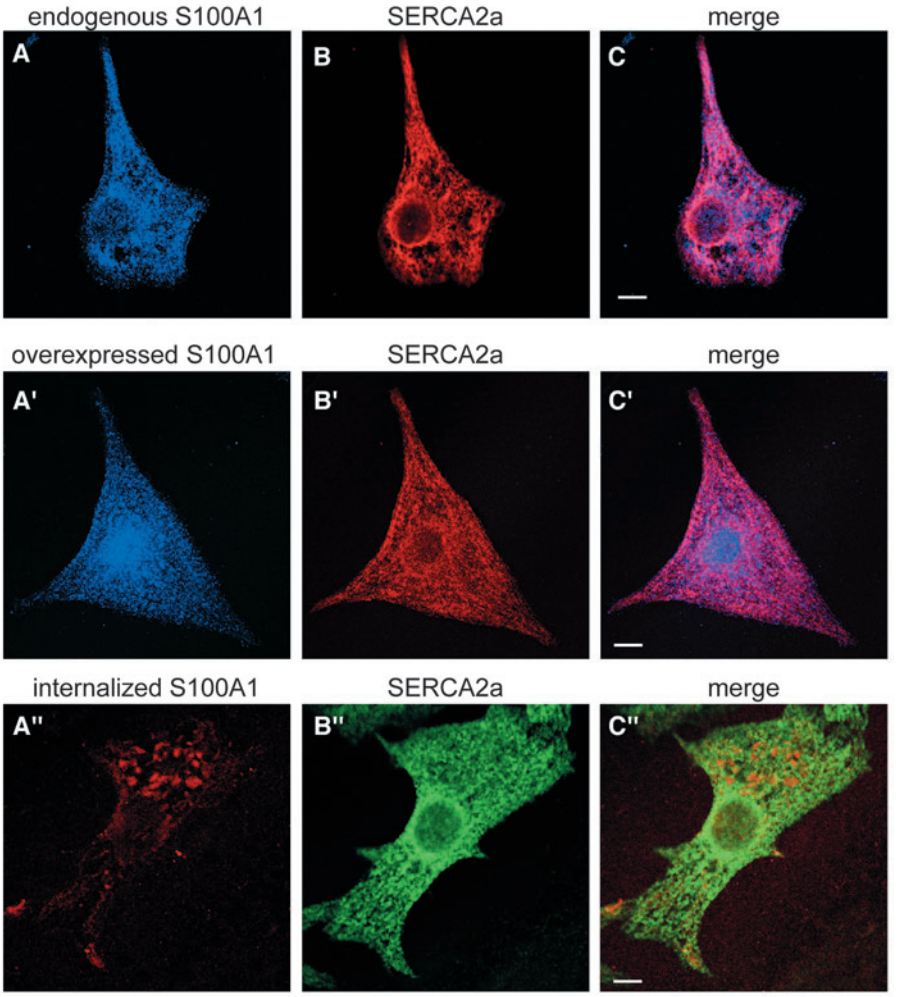

Fig. 3. Overexpressed but not internalized S100A1 colocalizes with SERCA2a at the SR. Immunolocalization of S100A1 and SERCA2a. (A) Endogenous S100A1 labeled with a monoclonal anti-S100A1/Cy5-anti-mouse antibody in control cells. (A') Overexpressed S100A1 detected with a polyclonal anti-human S100A1/Cy5–anti-rabbit antibody in AdS100A1-transduced NVCMs. (A'') Internalized Rh-S100A1. (B) Immunolabeling of SERCA2a in control, (B') AdS100A1-infected, (B'') and Rh-S100A1-treated NVCMs. (C) Overlay of A and B, and C', A' and B' depicts colocalization of endogenous and overexpressed S100A1 with SERCA2a (violet). (C'') Internalized Rh-S100A1 does not colocalize. Bar, 10 μm (C') and 5 μm (C,C'').

Overexpressed but not endocytosed S100A1 colocalizes with sarcoplasmic Ca^{2+}-regulatory proteins

We next examined whether the differential effect of overexpressed and internalized S100A1 on Ca^{2+}-turnover was associated with the distinct subcellular location of S100A1. Because S100A1 protein has previously been shown to co-immunoprecipitate with cardiac SR Ca^{2+}-regulatory proteins in human myocardium (Kiewitz et al., 2003), we examined the distribution of the SR Ca^{2+}-ATPase (SERCA2a) and its potential association with S100A1 in NVCMs with an increased level of S100A1 compared with control cells by immunolabeling with anti-SERCA2a antibodies (Fig. 3). To rule out that the adenoviral transduction procedure by itself caused a translocation of SERCA2a, we first established that its distribution in cells infected with a control virus was similar to that in uninfected NVCMs expressing only endogenous S100A1 (data not shown). Subsequently, the distribution of S100A1 in control cells (blue, Fig. 3A,C), in AdS100A1 NVCMs (blue, Fig. 3A',C') and in S100A1-treated cells (red, Fig. 3A'',C'') was compared to the location of immunolabeled SERCA2a (Fig. 3B,B',B''). Merging the corresponding confocal images clearly showed that overexpressed S100A1 and endogenous S100A1 partially colocalized with the SR Ca^{2+}-pump (violet, Fig. 3C,C'). Conversely, as illustrated in Fig. 3A'' to C'', internalized Rh-S100A1 protein (red) did not colocalize with the reticular distribution of SERCA2a (green).

In conclusion, the immunolocalization studies revealed that, depending on the experimental procedure used to increase S100A1 levels, S100A1 was routed to a different cellular compartment. Consequently, an association of S100A1 with the SR was only observed in AdS100A1-transduced NVCMs.

Enhanced Ca^{2+}-turnover in AdS100A1-transduced NVCMs is based on SR Ca^{2+}-cycling

Because overexpressed S100A1 was associated with SERCA2a at the SR, we tested the influence of SERCA2a

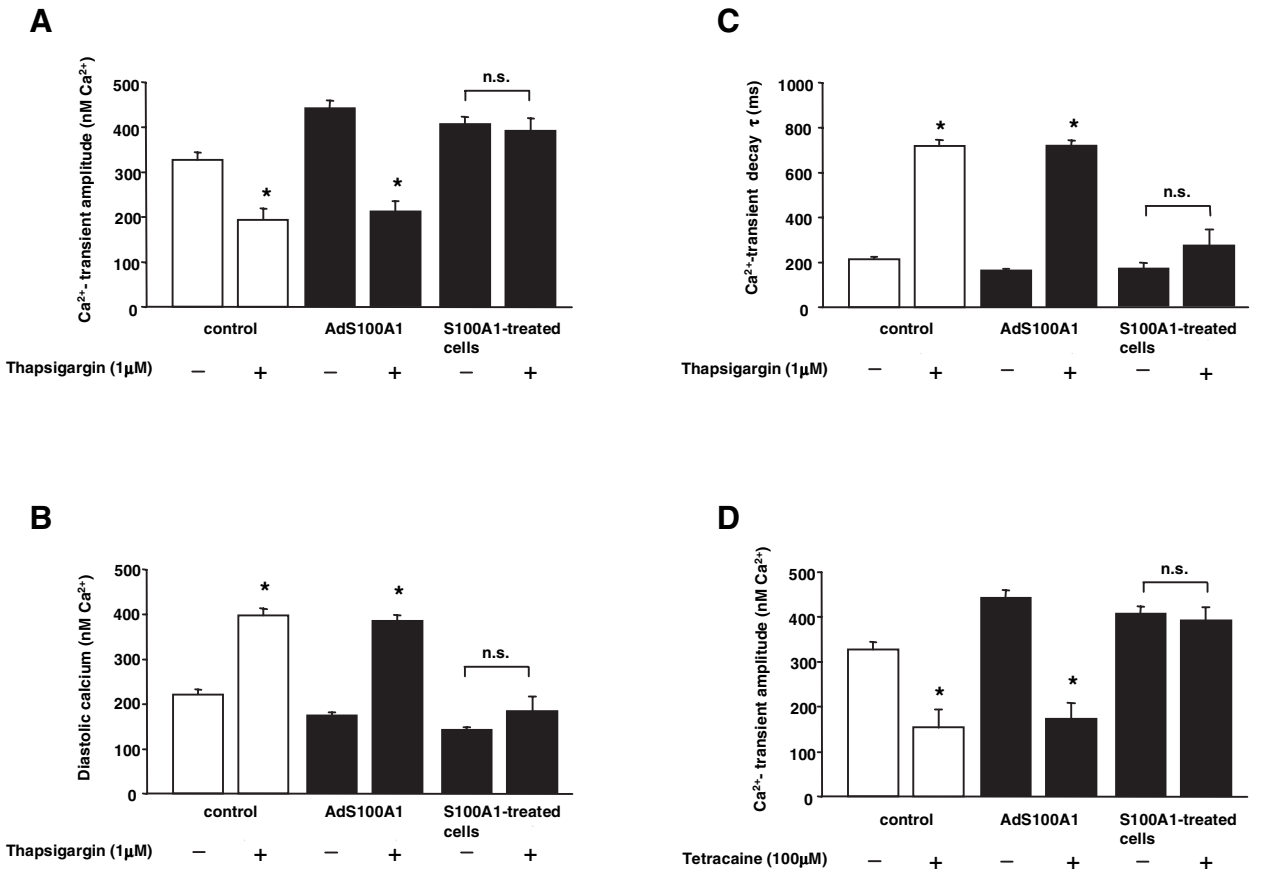

Fig. 4. Inhibition of SR Ca^{2+}-fluxes abolishes enhanced Ca^{2+}-cycling in S100A1-overexpressing but not in S100A1-treated NVCMs. (A) Addition of the SERCA2a inhibitor thapsigargin (1 μM) abolishes the S100A1-induced increase in the Ca^{2+}-transient amplitude in overexpressing (AdS100A1) but not S100A1-treated NVCMs. (B) Thapsigargin reduces diastolic $[Ca^{2+}]_i$ in control and S100A1-overexpressing cells, whereas S100A1-treated cells are not significantly affected. (C) SERCA2a inhibition raises the decay-constant τ in control and AdS100A1-infected NVCMs but does not significantly alter τ in S100A1-treated NVCMs. (D) Tetracaine (100 μM), an inhibitor of the SR Ca^{2+}-release channel (RyR), abrogates the increased Ca^{2+}-transient amplitude in S100A1-overexpressing NVCMs but does not significantly reduce the augmented amplitude of the Ca^{2+}-transient in S100A1-treated NVCMs relative to tetracaine-treated control cells. $*P<0.01$ vs. control. Measurements represent $n=150$ cells from three independent cell preparations. Data are given as mean±s.e.m.

antagonists on the efficiency of Ca^{2+}-cycling in AdS100A1- as well as in S100A1-treated NVCMs. Because Ca^{2+}-cycling in infected control cells and mock-treated NVCMs was indistinguishable, the two groups were pooled and are hereafter referred to as control NVCMs. As documented in Fig. 4A, a reduced amplitude in Ca^{2+}-transients of control NVCMs indicated that the SERCA2a-mediated Ca^{2+}-uptake into the SR was inhibited by thapsigargin (1 μM). Incubation of AdS100A1-cells with this SERCA2a inhibitor completely abolished the S1000A1-induced gain in the Ca^{2+}-transient amplitude (Fig. 4A). The Ca^{2+}-transients in thapsigargin-treated NVCMs did not significantly differ with respect to the diastolic Ca^{2+}-load or the decay rate between AdS100A1-transduced and control NVCMs: thapsigargin inhibition of SERCA2a equally raised diastolic $[Ca^{2+}]_i$ (Fig. 4B) and prolonged SR resequestration (Fig. 4C). By contrast, the enhancement of the Ca^{2+}-transient amplitude in S100A1-treated NVCMs was not affected by thapsigargin (Fig. 4A). Moreover, inhibition of SERCA2a had virtually no effect on the decreased diastolic $[Ca^{2+}]_i$ (Fig. 4B) and accelerated cytosolic Ca^{2+}-elimination (Fig. 4C) in S100A1-treated NVCMs. Like thapsigargin, inhibition of SR Ca^{2+}-release by tetracaine (100 μM), a blocker of the SR Ca^{2+}-release channel/ryanodine receptor (RyR2), decreased the amplitude of the Ca^{2+}-transient in control NVCMs and completely abolished the gain in the Ca^{2+}-transient amplitude in S1000A1-overexpressing NVCMs (Fig. 4D). However, tetracaine had no effect on the augmented Ca^{2+}-transient amplitude in S100A1-treated NVCMs (Fig. 4D). Consistent with these findings, immunofluorescence studies indicated that internalized S100A1 did not colocalize with SERCA2a (Fig. 3) or RyR2 (data not shown).

Because the data suggested that the increased efficiency of Ca^{2+}-turnover in S100A1-overexpressing but not in S100A1-treated NVCMs depended on SR Ca^{2+}-fluxes, we next investigated the SR Ca^{2+}-load in both groups. To address this issue, AdS100A1-infected and S100A1-treated NVCMs were exposed to caffeine (10 mM), and the amplitude of caffeine-releasable SR Ca^{2+} served as an indirect measure of the SR Ca^{2+}-content. As depicted in Fig. 5A, S100A1 overexpression caused an increase in the caffeine-induced Ca^{2+}-transient amplitude while internalized S100A1 apparently reduced the SR Ca^{2+}-load compared with the control.

Changes in NCX activity might be involved in modulating sarcolemmal Ca^{2+}-fluxes in response to S100A1

Cytosolic Ca^{2+}-turnover in NVCMs not only invokes the SR, but is simultaneously regulated by sarcolemmal Ca^{2+}-fluxes. The sodium-calcium exchanger (NCX) is a major regulator of sarcolemmal Ca^{2+}-fluxes. Analysis of the decay-constant τ of the caffeine-induced Ca^{2+}-transients, which served as a measure for NCX-mediated sarcolemmal Ca^{2+}-extrusion, revealed unchanged kinetics in AdS100A1-transduced NVCMs compared with cells infected with a control construct (Fig. 5B). Thus, it appears that overexpressed S100A1 does not affect NCX activity. Conversely, in S100A1-treated NVCMs τ of the caffeine-induced Ca^{2+}-transients was decreased compared with mock-treated NVCMs (control, Fig. 5). This finding indicated that the increased S100A1 level in the endosomal compartment could be responsible for the

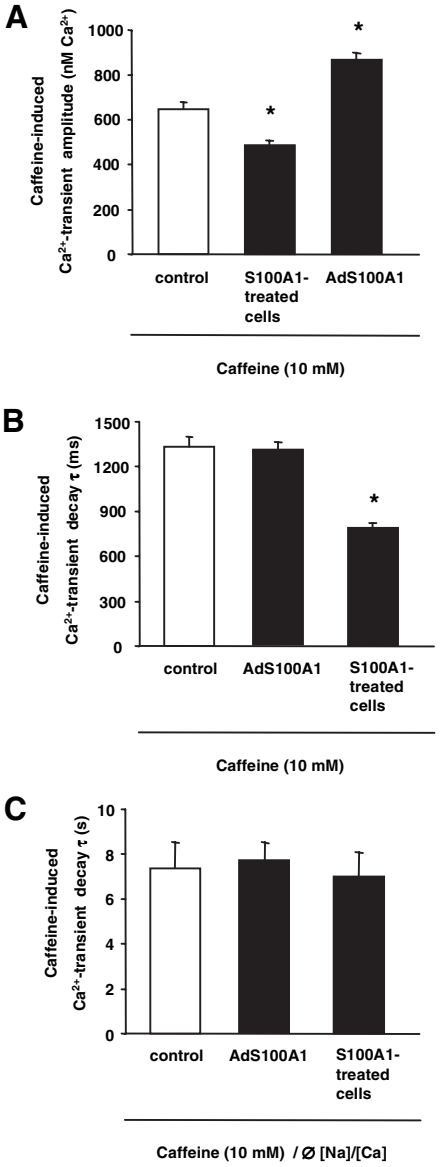

Fig. 5. Sarcolemmal Ca^{2+}-regulatory proteins modulate Ca^{2+}-cycling in S100A1-treated NVCMs. (A) Caffeine-induced Ca^{2+}-transient amplitudes reveal that overexpressed S100A1 (AdS100A1) enhances SR Ca^{2+}-content, whereas SR Ca^{2+}-levels are reduced in S100A1-treated cells compared with control cells exposed to caffeine. (B) The elimination of caffeine-releasable SR Ca^{2+} indicated by the decay-constant τ is similar in caffeine-treated control cells and S100A1-overexpressing cells. However, the decay of the Ca^{2+}-transient is accelerated in S100A1-treated NVCMs compared with control cells. (C) Switching to sodium/calcium-free medium abrogates decay acceleration in S100A1-treated cells. $*P<0.01$ vs. control. $n=50$ cells in AdS100A1 and S100A1-treated cells, control (mock- and Adcontrol-treated NVCMs) $n=100$ cells, cells from each group were obtained from three independent cell preparations. Data are given as mean±s.e.m.

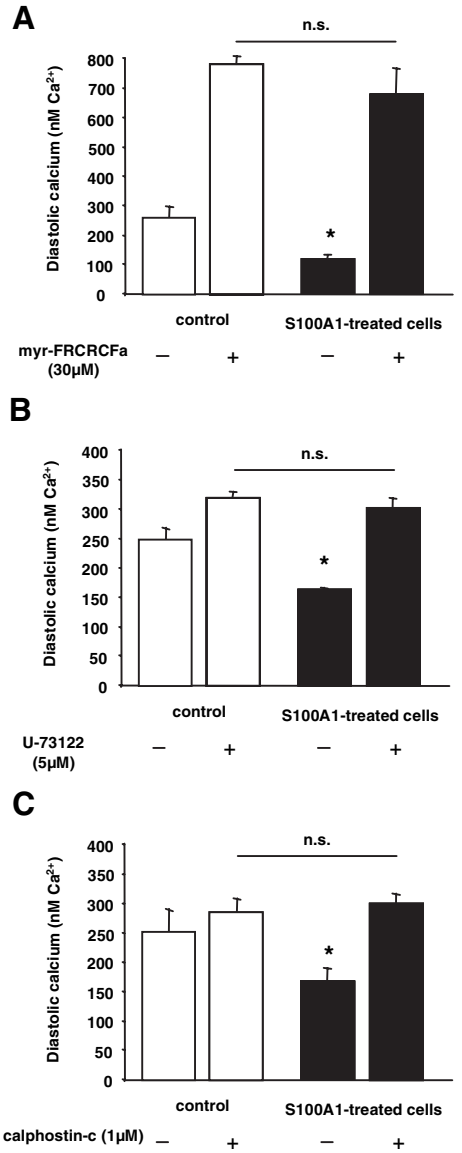

Fig. 6. Ca^{2+}-cycling in S100A1-treated NVCMs is regulated via PLC-PKC activation of NCX. (A) Inhibition of NCX activity by myr-FRCRCFa (30 μM) abrogated the S100A1-mediated decline in diastolic $[Ca^{2+}]_i$ in NVCMs. (B,C) The S100A1-mediated decrease in diastolic $[Ca^{2+}]_i$ is abolished trough inhibition of PLC and PK C by U-73122 and calphostin-c, respectively. $*P<0.01$ vs. control. Measurements represent $n=50$ cells from three independent cell preparations. Data are given as mean±s.e.m.

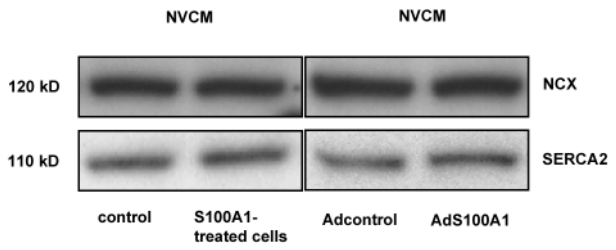

Fig. 7. Increased level of S100A1 does not alter expression of Ca^{2+}-regulatory proteins. Western blots of extracts from control, S100A1-treated, AdS100A1- and Adcontrol-transduced cells probed with specific antibodies. Levels of NCX and SERCA2a remain constant despite the increased levels of S100A1.

accelerated decay of the caffeine-mediated rise in cytosolic $[Ca^{2+}]_i$.

Because the NCX forward-mode mainly accounts for trans-sarcolemmal Ca^{2+}-efflux, the influence of NCX inhibition in S100A1-treated cells was studied. Selective NCX inhibition was achieved by rapidly replenishing the medium with sodium/calcium-free medium (Bassani et al., 1994; Despa et al., 2002). As documented by the caffeine-induced Ca^{2+}-transients in Fig. 5C, this regimen effectively abrogated the S100A1-mediated acceleration of the Ca^{2+}-transient decay.

This finding suggests that endocytosed S100A1 decreases diastolic $[Ca^{2+}]_i$ through enhanced sarcolemmal Ca^{2+}-extrusion, possibly involving an increased NCX forward-mode activity.

To further explore the influence of endocytosed S100A1 protein on NCX activity, we studied the impact of myristylated (myr)-FRCRCFa, a specific NCX blocker on diastolic $[Ca^{2+}]_i$ in S100A1-treated field-stimulated NVCMs. Myr-FRCRCFa is a novel, cell-permeable peptide inhibitor of NCX that alters neither L-type Ca^{2+}-channel/dihydropyridine receptor (LCC) nor Na^+- or K^+-channel activity, and appears to exhibit a higher degree of selectivity compared with other widely used NCX-inhibitors such as KB-R7943 or SEA0400 (Convery et al., 1998; Hobai et al., 1997; Khananshvili et al., 1995; Reuter et al., 2002). Administration of 30 μM myr-FRCRCFa caused a large rise in diastolic $[Ca^{2+}]_i$ in control cells and abrogated the S100A1-mediated decrease in diastolic $[Ca^{2+}]_i$ -treated cells (Fig. 6A).

Given that endocytosed S100A1 activates the PLC-PKC-p44/42 pathway (Most et al., 2003a) and PKC is known to stimulate NCX function (Iwamoto et al., 1996), we investigated whether triggering a corresponding pathway may be involved in increasing NCX activity in S100A1-treated NVCMs. Incubation with U73122 (5 μM), an inhibitor of PLC, resulted in a significant increase in diastolic $[Ca^{2+}]_i$ in S100A1-treated NVCMs (Fig. 6B). Similar results were obtained after addition of calphostin-c (1 μM), a PKC-inhibitor (Fig. 6C), indicating that enhanced cytosolic $[Ca^{2+}]_i$ removal by endocytosed S100A1 might involve PLC and PKC. Notably, PD98095 (10 μM) as well as myr-PKI (5 μM), specific inhibitors of the mitogen-activated protein kinase kinase MEK1 and protein kinase A (PKA), respectively, failed to inhibit the S100A1-mediated decrease in diastolic $[Ca^{2+}]_i$ (data not shown).

Increased S100A1 protein levels do not affect abundance of Ca^{2+}-regulatory proteins

Because increased S100A1 levels in NVCMs impinged on Ca^{2+}-regulatory proteins we assessed the abundance of NCX and SERCA protein in S100A1-treated and AdS100A1-transduced NVCMs. As shown by representative immunoblots in Fig. 7, neither endocytosis nor overexpression of S100A1 altered the levels of NCX and SERCA2a compared with control cells.

These findings suggest that the changes in Ca^{2+}-cycling seen in response to an increase of intracellular S100A1 are based on the altered activity of Ca^{2+}-regulatory proteins rather than their amounts.

Discussion

S100 Ca^{2+}-binding proteins have been associated with a variety of intracellular Ca^{2+}-mediated processes (Heizmann and Cox, 1998). Binding of Ca^{2+} induces a conformational change in the threedimensional structure and enables these proteins to interact with target proteins, thereby transducing the intracellular Ca^{2+}-signal (Wang et al., 2001). Recent findings involving *S100A1* gene transfer into ventricular cardiomyocytes have shown that S100A1 overexpression enhances cytosolic Ca^{2+}-cycling and contractile properties both in vitro and in vivo (Most et al., 2001; Most et al., 2003b; Most et al., 2003c; Remppis et al., 2002; Remppis et al., 2004). Consistently, S100A1-deficient mice display an impaired cardiac contractility in response to hemodynamic stress (Du et al., 2002). These studies promote S100A1 as a novel key regulator of cardiac function. In addition, recent studies from our laboratory provide evidence that S100A1 may also act on ventricular cardiomyocytes through an unrelated mechanism: uptake of S100A1 from the extracellular environment protects cells from apoptosis induced by reactive oxygen species or 2-deoxyglucose (Most et al., 2003a). This downstream effect apparently relies on RAGE-indepedent endocytosis of extracellular S100A1 and involves the activation of the PLC-PKC-ERK1/2 prosurvival pathway. Several studies support the notion that extracellular S100 proteins may have distinct functions in cellular physiology and pathology. For example, S100A4 was reported to stimulate the outgrowth of neurite cells (Novitskaya et al., 2000), whereas S100B has been shown to be involved in the regulation of cell differentiation and survival (Huttunen et al., 2000; Sorci et al., 2003; Sorci et al., 2004a; Sorci et al., 2004b). Another example is S100A12, which has been implicated as an important pro-inflammatory regulator in numerous chronic inflammatory diseases (Foell et al., 2003a; Foell et al., 2003b; Foell et al., 2003c; Foell et al., 2003d). Notably, release of S100A1 into the extracellular space in reponse to ischemic cadiac injury has been reported (Kiewitz et al., 2000), but it is unclear whether extracellular S100A1 might affect Ca^{2+}-homeostasis in ventricular cardiomyocytes. In the present study we addressed this issue by comparing the effects of S100A1 added to the extracellular environment to the effects of adenoviral-mediated S100A1 overexpression on cardiac Ca^{2+}-cycling in vitro.

The model illustrated in Fig. 8 summarizes the data presented in this paper. First, we show that recombinant S100A1 added to the extracellular environment is internalized

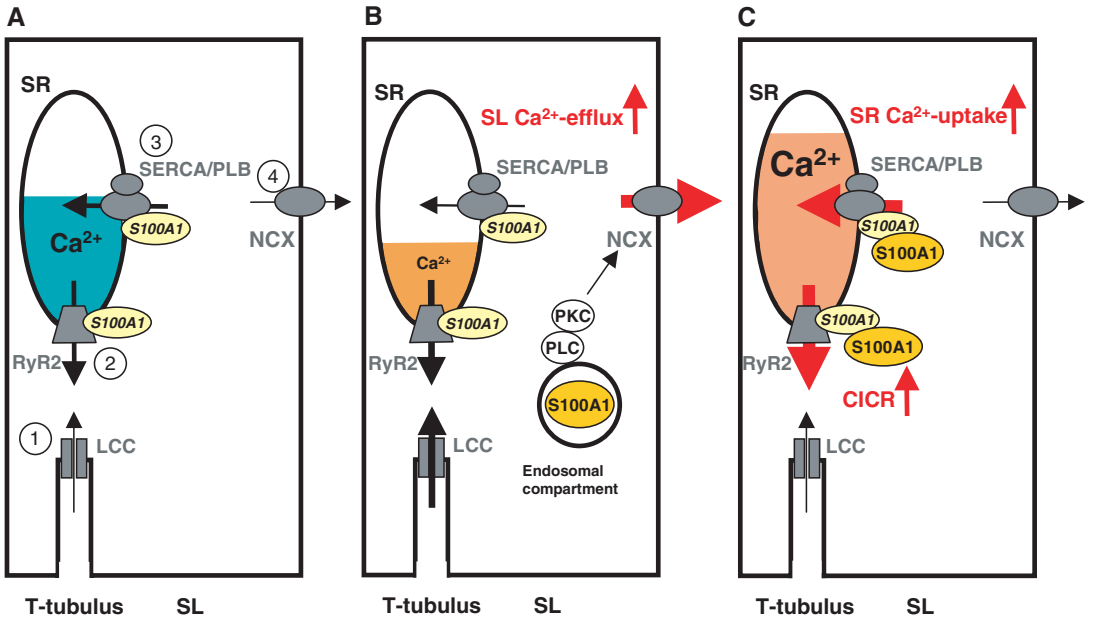

Fig. 8. Differential effects of endocytosed and overexpressed S100A1 on sarcolemmal and sarcoplasmic Ca^{2+}-cycling. (A) Simplified scheme of intracellular Ca^{2+}-fluxes in a ventricular cardiomyocyte. Endogenous S100A1 (hatched oval) is located at the SR where it interacts with SERCA2a and RyR2. (1) Electrical depolarization of the transverse tubule membrane (T-tubulus) activates inward Ca^{2+}-flux through L-type voltage-gated Ca^{2+}-channels (LCC), which (2) triggers the release of Ca^{2+} from SR stores via ryandine receptors (RyR2). As a result, contractile filaments are activated. (3) For relaxation to occur, the cytosolic $[Ca^{2+}]_i$ must decline. This process is mainly mediated by the SR Ca^{2+}-ATPase (SERCA2a), which resequesters cytosolic Ca^{2+} in the SR. (4) At the sarcolemma, Ca^{2+} is extruded primarily via the sodium-calcium exchanger (NCX). (B) Extracellularly added S100A1 is internalized and subsequently routed to the endosomal compartment, where it increases the activity of PLC and PKC (both associated with the endosomal compartment). Through activation of this signaling pathway, internalized S100A1 eventually modulates intracellular Ca^{2+}-flux through an enhanced sarcolemmal Ca^{2+}-extrusion via NCX. The increased Ca^{2+}-extrusion leads to a decreased SR Ca^{2+}-load. (C) Effects of overexpressed S100A1 on the intracellular Ca^{2+}-cycling. Overexpressed S100A1 is located at the SR, where it associates with the SR-regulatory proteins SERCA2a and RyR2. As a result, intracellular Ca^{2+}-cycling is enhanced leading to an increased SR Ca^{2+}-uptake and SR Ca^{2+}-load. This, in turn, gives rise to an enhanced Ca^{2+}-induced SR Ca^{2+}-release (CICR).

and subsequently modulates cytosolic Ca^{2+}-cycling in ventricular cardiomyocytes (Fig. 8B). Second, compared with the effects of adenoviral-mediated S100A1 overexpression on Ca^{2+}-turnover (Fig. 8C), internalized S100A1 modulates Ca^{2+}-homeostasis in a different manner, which is likely to involve the NCX. The immunofluorescence studies suggest that this mechanistic difference is related to a distinct subcellular location of internalized versus overexpressed S100A1. Both experimental regimens, endocytosis of extracellularly added S100A1 and intracellular S100A1 overexpression led to a three-to-fourfold increase of intracellular levels of the Ca^{2+}-sensor protein. Because the increase in intracellular S100A1 is comparable, we can largely rule out that the total amount of S100A1 is responsible for the differential effects on cytosolic Ca^{2+}-turnover. S100A1 uptake was found to enhance the cytosolic Ca^{2+}-transient amplitude by a marked decrease in diastolic $[Ca^{2+}]_i$, while systolic $[Ca^{2+}]_i$ were mostly unchanged. By contrast, overexpression of S100A1 enhanced the Ca^{2+}-transient amplitude mainly by a marked increase in systolic $[Ca^{2+}]_i$ in combination with a slight decrease in diastolic $[Ca^{2+}]_i$. The downstream effect of extracellularly added S100A1 on cardiac Ca^{2+}-handling together with the previously demonstrated cardioprotective effects argue that S100A1 could act as paracrine cardiac factor which also acts on other cardiac cells, such as fibroblasts, smooth muscle and endothelial cells.

Along with a differential Ca^{2+}-handling, we also observed a different location of S100A1 that was taken up from the extracellular environment compared with overexpressed S100A1. The latter is associated with the SR since it colocalized with the SR Ca^{2+}-regulatory proteins SERCA2a (Fig. 8C) and RyR2 (data not shown). These findings are in line with recently published data showing Ca^{2+}-dependent co-immunoprecipitation of endogenous S100A1 protein with RyR2 and SERCA2a in murine and human myocardium (Kiewitz et al., 2003; Most et al., 2003b). Like Kiewitz et al., who were able to show a colocalization of endogenous S100A1 and SERCA2a in neonatal cardiomyocytes from mouse (Kiewitz et al., 2003), our data reveal a colocalization in rat neonatal cardiomyocytes. Consistently, when RyR2 and SERCA2a activities were inhibited in S100A1-overexpressing cells, the amplitude of Ca^{2+}-transients display a marked decrease; also, diastolic $[Ca^{2+}]_i$ are noticeably increased and the decay of Ca^{2+}-transients is decelerated (Fig. 8C). By contrast, inhibitors of SERCA2a or RyR2 neither affected the S100A1-induced increase in the Ca^{2+}-transient amplitude nor lowered diastolic $[Ca^{2+}]_i$ in cardiomyocytes following uptake of extracellular S100A1. Thus, enhanced Ca^{2+}-cycling in cardiomyocytes overexpressing S100A1 is presumably based on SR Ca^{2+}-cycling. These findings are consistent with previous studies showing that overexpressed S100A1 increased

both SR Ca^{2+}-uptake and Ca^{2+}-load, as well as Ca^{2+}-release from the SR (Most et al., 2001; Most et al., 2003b; Remppis et al., 2002). Because the levels of SERCA2a were unaltered, we conclude that overexpressed S100A1 enhances SR Ca^{2+}-load by an increased SERCA2a activity rather than protein abundance.

Internalized S100A1, however, does not colocalize with SR Ca^{2+}-regulatory proteins (Fig. 3) and was also not detected at the sarcolemmal membrane of cardiomyocytes (Most et al., 2003a). Instead, it displays a vesicular-like perinuclear distribution that has recently been identified as part of the endosomal compartment (Most et al., 2003a). Consistent with the distinct location of S100A1, Ca^{2+}-handling by S100A1-treated cells appears to be independent of SR Ca^{2+}-regulatory proteins (Fig. 8B). However, since S100A1 uptake decreased the SR Ca^{2+}-levels, another mechanism must be affected that accounts for an enhanced cytosolic Ca^{2+}-elimination. Accordingly, we measured an accelerated decay of the caffeine-induced Ca^{2+}-transient amplitude, which indicates that the enhanced cytosolic Ca^{2+}-elimination is likely to involve a trans-sarcolemmal Ca^{2+}-efflux via NCX. In addition, inhibition of NCX by switching to sodium/calcium-free medium abolished this effect, which supports the notion that internalized S100A1 stimulates cytosolic Ca^{2+}-extrusion through the NCX forward-mode rather than through the slow Ca^{2+}-removal systems such as the plasma membrane Ca^{2+}-ATPase (PMCA) and the mitochondrial uniporter (Bassani et al., 1994). Similar effects were seen in S100A1-treated field-stimulated cardiomyocytes in the presence of the specific NCX inhibitor myr-FRCRCFa. The inhibitory cell-permeable hexapeptide abolished the S100A1-mediated decrease in diastolic $[Ca^{2+}]_i$. On the basis of these results, we propose a mechanism where endocytosed S100A1 decreases diastolic $[Ca^{2+}]_i$ by activating sarcolemmal Ca^{2+}-extrusion via NCX.

Because endocytosed S100A1 was not present at the sarcolemmal membrane, the question arose, how an increased S100A1 protein level confined to the endosomal compartment could trigger NCX activity. However, it has been shown that PKC and PLC play a role in the regulation of NCX in neonatal cardiomyocytes (Iwamoto et al., 1996). Moreover, we have shown that internalized S100A1 activates the ERK1/2 signaling pathway through activation of PLC and PKC (Most et al., 2003a). These findings and our Ca^{2+}-transient measurements in the presence of specific inhibitors of PLC and PKC prompted us to suggest that a S100A1-mediated activation of NCX forward mode might occur through the PLC and PKC signaling pathway.

In conclusion, our data indicates that the enhanced Ca^{2+}-cycling observed in S100A1-overexpressing cardiomyocytes predominantly involves SR Ca^{2+}-fluxes (Fig. 8C), whereas endocytosed S100A1 apparently alters intracellular Ca^{2+}-turnover through sarcolemmal modulation (Fig. 8B). According to the model, accumulation of internalized S100A1 in the endosomal compartment somehow triggers endosome-associated PLC and PKC, which then activate NCX to increase sarcolemmal Ca^{2+}-efflux.

This study provides the first insight into the mechanisms through which S100A1 differentially modulates sarcolemmal and sarcoplasmic Ca^{2+}-handling in ventricular cardiomyocytes depending on the subcellular location of this protein. Endosomal S100A1 protein appears to modulate Ca^{2+}-cycling through an enhanced NCX forward-mode activity, whereas cytosolic S100A1 increases Ca^{2+}-cycling by enhancing SR Ca^{2+}-fluxes. The latter is likely to underlie the positive inotropic and lusitropic effects seen in S100A1-overexpressing myocardium (Most et al., 2001; Most et al., 2003b; Remppis et al., 2002; Remppis et al., 2004). In addition, we have very recently shown that cardiac adenoviral *S100A1* gene delivery rescues failing myocardium in vitro and in vivo (Most et al., 2004), which warrants further studies on the impact of decreased diastolic $[Ca^{2+}]_i$ and SR Ca^{2+}-load resulting from S100A1 endocytosis on cardiac function in vivo.

This work was supported in part by grants from the University of Heidelberg to P.M. (Forschungsförderung 93/2002 and 61/2003), the Deutsche Forschungsgemeinschaft (DFG) to P.M. (Mo 1066/1-1) and T.W. (We 2366/3-1), from the M. E. Müller Foundation of Switzerland and the Kanton of Basel Stadt (to M.B., U.A. and C.-A. S.) and the National Institute of Health to W.J.K. (R01-HL59533 and R01-HL56205).

References

Barger, S. W. and van Eldik, L. J. (1992). S100 beta stimulates calcium fluxes in glial and neuronal cells. *J. Biol. Chem.* **267**, 9689-9694.

Bassani, J. W. M., Bassani, R. A. and Bers, D. M. (1994). Relaxation in rabbit and rat cardiac cells: species-dependent differences in cellular mechanisms. *J. Physiol.* **476**, 279-293.

Convery, M. K., Levi, A. J., Khananshvili, D. and Hancox, J. C. (1998). Actions of myristyl-FRCRCFa, a cell-permeant blocker of the cardiac sarcolemmal Na-Ca exchanger, tested in rabbit ventricular myocytes. *Pflugers Arch.* **436**, 581-590.

Despa, S., Islam, M. A., Pogwizd, S. M. and Bers, D. M. (2002). Intracellular [Na+] and Na+ pump rate in rat and rabbit ventricular myocytes. *J. Physiol.* **539**, 133-143.

Donato, R. (2003). Intracellular and extracellular roles of S100 proteins. *Microsc. Res. Tech.* **60**, 540-551.

Foell, D., Ichida, F., Vogl, T., Yu, X., Chen, R., Miyawaki, T., Sorg, C. and Roth, J. (2003a). S100A12 (EN-RAGE) in monitoring Kawasaki disease. *Lancet* **361**, 1270-1272.

Foell, D., Kane, D., Bresnihan, B., Vogl, T., Nacken, W., Sorg, C., Fitzgerald, O. and Roth, J. (2003b). Expression of the pro-inflammatory protein S100A12 (EN-RAGE) in rheumatoid and psoriatic arthritis. *Rheumatology* **42**, 1383-1389.

Foell, D., Kucharzik, T., Kraft, M., Vogl, T., Sorg, C., Domaschke, W. and Roth, J. (2003c). Neutrophil derived S100A12 (EN-RAGE) is strongly expressed during chronic active inflammatory bowel disease. *Gut* **52**, 847-853.

Foell, D., Seeliger, S., Vogl, T., Koch, H. G., Maschek, H., Harms, E., Sorg, C. and Roth, J. (2003d). Expression of S100A12 (EN-RAGE) in cystic fibrosis. *Thorax* **58**, 613-617.

Haimoto, H. and Kato, K. (1988). S100a0 (alpha alpha) protein in cardiac muscle. Isolation from human cardiac muscle and ultrastructural localization. *Eur. J. Biochem.* **171**, 409-415.

Heizmann, C. W. and Cox, J. A. (1998). New perspectives on S100 proteins: a multi-functional Ca(2+)-, Zn(2+)- and Cu(2+)-binding protein family. *Biometals* **11**, 383-397.

Hobai, I. A., Khananshvili, D. and Levi, A. J. (1997). The peptide "FRCRCFa", dialysed intracellularly, inhibits the Na/Ca exchange in rabbit ventricular myocytes with high affinity. *Pflugers Arch.* **433**, 455-463.

Hofmann, M. A., Drury, S., Fu, C., Qu, W., Taguchi, A., Lu, Y., Avila, C., Kambham, N., Bierhaus, A., Nawroth, P. et al. (1999). RAGE mediates a novel proinflammatory axis: a central cell surface receptor for S100/calgranulin polypeptides. *Cell* **97**, 889-901.

Huttunen, H. J., Kuja-Panula, J., Sorci, G., Agneletti, A. L., Donato, R. and Rauvala, H. (2000). Coregulation of neurite outgrowth and cell survival by amphoterin and S100 proteins through receptor for advanced glycation end products (RAGE) activation. *J. Biol. Chem.* **275**, 40096-40105.

Iwamoto, T., Pan, Y., Wakabayashi, S., Imagawa, T., Yamanaka, H. I. and Shigekawa, M. (1996). Phosphorylation-dependent regulation of cardiac

Na+/Ca2+ exchanger via protein kinase C. *J. Biol. Chem.* **271**, 13609-13615.

Kato, K. and Kimura, S. (1985). S100ao (alpha alpha) protein is mainly located in the heart and striated muscles. *Biochim. Biophys. Acta* **842**, 146-150.

Khananshvili, D., Shaulov, G., Weil-Maslansky, E. and Baazov, D. (1995). Positively charged cyclic hexapeptides, novel blockers for the cardiac sarcolemma Na(+)-Ca2+ exchanger. *J. Biol. Chem.* **270**, 16182-16188.

Kiewitz, R., Acklin, C., Minder, E., Huber, P. R., Schafer, B. W. and Heizmann, C. W. (2000). S100A1, a new marker for acute myocardial ischemia. *Biochem. Biophys. Res. Commun.* **274**, 865-871.

Kiewitz, R., Acklin, C., Schafer, B. W., Maco, B., Uhri, K. B., Wuytack, F., Erne, P. and Heizmann, C. W. (2003). Ca(2+)-dependent interaction of S100A1 with the sarcoplasmic reticulum Ca(2+)-ATPase2a and phospholamban in the human heart. *Biochem. Biophys. Res. Commun.* **306**, 550-557.

Kubista, H., Donato, R. and Hermann, A. (1999). S100 calcium binding protein affect neuronal electrical discharge activity by modulation of potassium currents. *Neuroscience* **90**, 493-508.

Mikkelsen, S. E., Novitskaya, V., Kriajevska, M., Berezin, V., Bock, E., Norrild, B. and Lukanidin, E. (2001). S100A12 protein is a strong inducer of neurite outgrowth from primary hippocampal neurons. *J. Neurochem.* **79**, 767-776.

Most, P., Bernotat, J., Ehlermann, P., Pleger, S. T., Reppel, M., Borries, M., Niroomand, F., Pieske, B., Janssen, P. M., Eschenhagen, T. et al. (2001). S100A1: a regulator of myocardial contractility. *Proc. Natl. Acad. Sci. USA* **98**, 13889-13894.

Most, P., Boerries, M., Eicher, C., Schweda, C., Ehlermann, P., Pleger, S. T., Löffler, E., Koch, W. J., Katus, H. A., Schoenenberger, C. A. et al. (2003a). Extracellular S100A1 protein inhibits apoptosis in ventricular cardiomyocytes via activation of the extracellular-regulated kinase (ERK1/2) pathway. *J. Biol. Chem.* **278**, 48404-48412.

Most, P., Remppis, A., Pleger, S. T., Löffler, E., Ehlermann, P., Bernotat, J., Kleuss, C., Heierhorst, J., Ruiz, P., Witt, H. et al. (2003b). Transgenic overexpression of the Ca2+ binding protein S100A1 in the heart leads to increased in vivo myocardial contractile performance. *J. Biol. Chem.* **278**, 33809-33817.

Most, P., Remppis, A., Weber, C., Bernotat, J., Ehlermann, P., Pleger, S. T., Kirsch, W., Weber, M., Uttenweiler, D., Smith, G. L. et al. (2003c). The C-terminus (aa 75-94) and the linker region (aa 42-54) of the Ca2+ binding protein S100A1 differentially enhance sarcoplasmic Ca2+ release in murine skinned skeletal muscle fibres. *J. Biol. Chem.* **278**, 26356-26364.

Most, P., Pleger, S., Völkers, M., Heidt, B., Boerries, M., Weichenhan, D., Löffler, E., Janssen, P. M., Eckhart, A. D., Martini, J. et al. (2004). Cardiac adenoviral S100A1 gene transfer rescues failing myocardium. *J. Clin. Invest.* **114**, 1550-1563.

Novitskaya, V., Grigorian, M., Kriajevska, M., Tarabykina, S., Bronstein, I., Berezin, V., Bock, E. and Lukanidin, E. (2000). Oligomeric forms of the metastasis-related Mts1 (S100A4) protein stimulate neuronal differentiation in cultures of rat hippocampal neurons. *J. Biol. Chem.* **275**, 41278-41286.

Rammes, A., Roth, J., Goebeler, M., Klempt, M., Hartmann, M. and Sorg, C. (1997). Myeloid-related protein (MRP) 8 and MRP14, calcium-binding proteins of the S100 family, are secreted by activated monocytes via a novel, tubulin-dependent pathway. *J. Biol. Chem.* **272**, 9496-9502.

Remppis, A., Most, P., Löffler, E., Ehlermann, P., Bernotat, J., Pleger, S. T., Börries, M., Repper, M., Fischer, J., Koch, W. J. et al. (2002). The small EF-hand Ca^{2+} binding protein S100A1 increases contractility and Ca^{2+} cycling in rat cardiac myocytes. *Basic Res. Cardiol.* **97**, 56-62.

Remppis, A., Pleger, S. T., Most, P., Lindenkamp, J., Ehlermann, P., Löffler, E., Weil, J., Eschenhagen, T., Koch, W. J. and Katus, H. A. (2004). S100A1 gene transfer: A strategy to strenghten engineered cardiac grafts. *J. Gene Med.* **6**, 387-394.

Reuter, H., Henderson, S. A., Han, T., Matsuda, T., Baba, A., Ross, R. S., Goldhaber, J. I. and Philipson, K. D. (2002). Knockout mice for pharmacological screening. testing the specificity of Na-Ca exchange inhibitors. *Circ. Res.* **91**, 90-92.

Selinfreund, R. H., Barger, S. W., Pledger, W. J. and van Eldik, L. J. (1991). Neurotrophic protein S100 beta stimulates glial cell proliferation. *Proc. Natl. Acad. Sci. USA* **88**, 3554-3558.

Sorci, G., Riuzzi, F., Agneletti, A. L., Marchetti, C. and Donato, R. (2003). S100B inhibits myogenic differentiation and myotube formation in a RAGE-independent manner. *Mol. Cell. Biol.* **23**, 4870-4881.

Sorci, G., Riuzzi, F., Agneletti, A. L., Marchetti, C. and Donato, R. (2004a). S100B causes apoptosis in a myoblast cell line in a RAGE-independent manner. *J. Cell. Physiol.* **199**, 274-283.

Sorci, G., Riuzzi, F., Arcuri, C., Giambanco, I. and Donato, R. (2004b). Amphotericin stimulates myogenesis and counteracts the antimyogenic factors basic fibroblast growth factor and S100B via RAGE binding. *Mol. Cell. Biol.* **24**, 4880-4894.

Wang, Z., Zhang, H., Ding, Y., Wang, G., Wang, X., Ye, S., Bartlam, M., Tang, H., Liu, Y., Jiang, F. et al. (2001). Preliminary X-ray crystallographic analysis of a Ca2+-binding protein human S100A1. *Acta Crystallogr. D Biol. Crystallogr.* **57**, 882-883.

Zimmer, D. B., Cornwall, E. H., Landar, A. and Song, W. (1995). The S100 protein family: history, function, and expression. *Brain Res. Bull.* **37**, 417-429.